Non-local quantum criticality in Ce(Ru1-xFex)2Ge2 (x=xc=0.76)

Montfrooij, W.; Aronson, M.; Rainford, B.D.; Mydosh, J.A.; Murani, A.P.; Haen, P.; Fukuhara, T.

Extended versus Local Fluctuations in Quantum Critical $Ce(Ru_{1-x}Fe_x)_2Ge_2$ ($x = x_c = 0.76$)

W. Montfrooij,[1] M. C. Aronson,[1] B. D. Rainford,[2] J. A. Mydosh,[3] A. P. Murani,[4] P. Haen,[5] and T. Fukuhara[6]

[1]*University of Michigan, Ann Arbor, Michigan 48109, USA*
[2]*University of Southampton, Southampton SO17 1BJ, United Kingdom*
[3]*Leiden University, 2300 RA Leiden, The Netherlands*
[4]*Institute Laue-Langevin, BP 156, 38042, Genoble cedex 9, France*
[5]*CRTBT, CNRS, BP 166, 38042 Grenoble cedex 9, France*
[6]*Faculty of Engineering, Toyama Prefectural University, Toyama 939-0398, Japan*

(Received 19 July 2002; published 19 August 2003)

We present inelastic neutron scattering experiments, performed near the antiferromagnetic quantum critical point in $Ce(Ru_{0.24}Fe_{0.76})_2Ge_2$. Both local and long-range fluctuations of the local moments are observed, but due to the Kondo effect only the latter are critical. We propose a phenomenological expression which fits the energy E, temperature T, and wave vector q dependences of the dynamic susceptibility, describing the non-Fermi liquid E/T scaling found at every q.

DOI: 10.1103/PhysRevLett.91.087202 PACS numbers: 75.30.Fv, 71.27.+a, 75.40.Gb

The stability of magnetic order among moments exchange coupled to the conduction electrons in a metal arises from the dynamic competition of two forces: the Kondo compensation of the moments and their long-range RKKY interaction, both depending on the exchange interaction J. Experimental evidence [1,2] shows that magnetic order is initially stabilized by increasing J, but that ultimately magnetic order terminates at a zero temperature quantum critical point (QCP) for a critical value J_c, yielding a magnetically enhanced but paramagnetic Fermi liquid phase for larger J.

Two scenarios have been proposed to explain this generic phase diagram. In the first [3,4], magnetic order at the QCP is a spin density wave (SDW) instability of the Fermi surface, as it is preceded by moment compensation below a Kondo temperature T_K which is finite at $J = J_c$. Here, only the long wavelength fluctuations of the order parameter are critical, leading to Lorentzian energy and wave vector dependences in the vicinity of the ordering wave vector $\vec{Q}$ [3,4]. An example of such a system is $Ce_{0.87}La_{0.13}Ru_2Si_2$ [5]. In the second view [6–8], both T_K and the magnetic ordering temperature are zero at the QCP. Complete Kondo compensation of moments is thus possible only in the paramagnetic phase for $J > J_c$. Magnetic order ($J < J_c$) consequently involves moments which are both long-lived and spatially localized. Here, the competition between Kondo screening and long-range order leads to local as well as long wavelength degrees of freedom, and both can be critical near the QCP. The experimental signatures of this latter scenario are an anomalous energy dependence for all q [8], as well as the absence of Kondo compensation at any T when $J = J_c$.

It is difficult to distinguish the two views since experiments are necessarily done at finite T on materials with disorder. Inelastic neutron scattering (INS) experiments, carried out on two QCP systems, $CeCu_{5.9}Au_{0.1}$ [7] and $UCu_{5-x}Pd_x$ ($x = 1, 1.5$) [9,10], have provided key information about the onset of dynamical and spatial correlations near the QCP. Localized magnetic moments are present in both materials, while the modulation of the static susceptibility χ_q reveals the presence of magnetic interactions among these moments. Different arguments are presented for the two materials which support the view that the local degrees of freedom and not the long-range coupling control the critical behavior. Direct comparison of χ_q at different T in $UCu_{5-x}Pd_x$ ($x = 1, 1.5$) [9] shows that the interactions are almost T independent, while the local susceptibility diverges as $T \to 0$. Excitations at every q display anomalous E dependences as well as E/T scaling.

A different depiction of quantum critical behavior is found in $CeCu_{5.9}Au_{0.1}$, where the commensurate roles of T, E, and q in tuning the dynamic susceptibility $\chi(q, E, T)$ to criticality are reflected in a generalized Curie-Weiss expression [7], $\chi(q, E, T)^{-1} \sim \theta_q^\alpha + (iaE + T)^\alpha$. While the longest lived and longest ranged fluctuations occur for $\vec{q} = \vec{Q}$, anomalous E and T dependences are found at every q, as well as E/T scaling when $\theta_{q=Q} = 0$. Si *et al.* [8] argue that the $T = 0$ phase transition in $CeCu_{5.9}Au_{0.1}$ is actually driven by fluctuations on the shortest length scales, providing an operational definition of local criticality.

We present INS results on $Ce(Ru_{0.24}Fe_{0.76})_2Ge_2$, which has been doped to an antiferromagnetic (AF) QCP. The localized moments present in this system experience substantial Kondo compensation. Both local and long wavelength fluctuations are found at all T, although only the latter are truly critical. The non-Fermi liquid (nFl) E/T scaling is found at all T and q, but neither the generalized Curie-Weiss expression [7] nor the Lorentzians of the SDW model [4,5] describe our data. We propose instead a new phenomenological expression for $\chi(q, E, T)$ which is critical only on the longest length scales. Accordingly, we argue that $Ce(Ru_{0.24}Fe_{0.76})_2Ge_2$ is the first example of a new type of quantum critical system.

The phase diagram obtained from both pressurization [11] and Fe doping studies of $CeRu_2Ge_2$ [Fig. 1(a)] fulfills the basic requirement for the SDW scenario, displaying an AF QCP accompanied by a finite T_K. Below $T = 8$ K, $CeRu_2Ge_2$ is a ferromagnet (FM) [12–14]. Under pressure p, FM is supplanted by two AF phases, which in turn vanish at $p_c = 67$ kbar. Substantial moment compensation is observed at p_c, where T_K is estimated to be $\sim$15 K. Further increasing p stabilizes a Fermi liquid phase over an expanding T range. INS experiments cannot be performed at high p, so it is significant that a similar sequence of phases is observed in the doping series $Ce(Ru_{1-x}Fe_x)_2Ge_2$ [Fig. 1(a)] and in the Ising system $CeRu_2(Si_{1-x}Ge_x)_2$ [11,14]. The FM phase boundary [12] is only qualitatively reproduced by the resistivity data, but the AF phase boundary, taken from our ac and dc susceptibility measurements, reproduces the pressure results. The AF QCP occurs for a critical Fe concentration $x_c = 0.76 \pm 0.05$, slightly below the previous [12] estimate.

We prepared a 30 g polycrystalline sample of $Ce(Ru_{0.24}Fe_{0.76})_2Ge_2$ by arc melting, followed by a two week anneal at 1000 ° C. Microprobe and electron backscattering measurements verified that the composition is $x = 0.76 \pm 0.02$. Isolated regions of a $CeGe_2$ impurity phase occupy less than 2% of the sample volume. Neutron diffraction experiments found AF correlations below 5 K, but no bulk phase transition was observed down to 0.4 K in specific heat measurements. The latter show a log$T$ dependence between 0.5 and 10 K, with $c_p/T = 0.63\ \mathrm{J\,K^{-2}\,mol^{-1}}$ at 0.5 K [15]. Thus, our sample is very close to x_c.

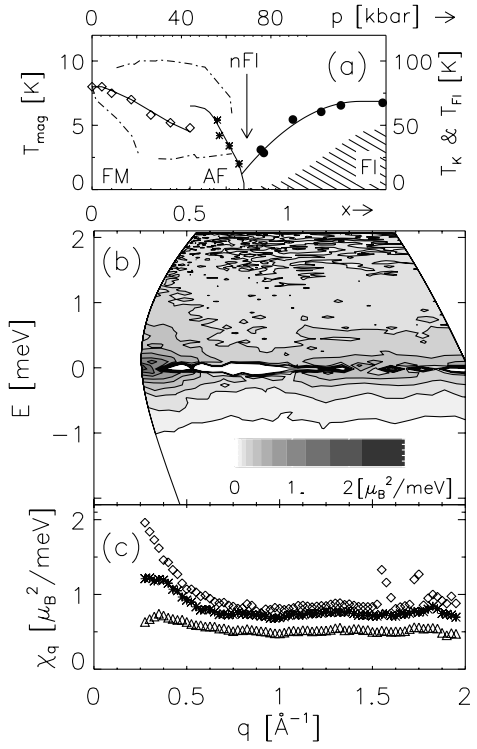

FIG. 1. (a) The magnetic phase diagram for $CeRu_2Ge_2$ versus pressure [11] (dashed lines) and Fe doping (◇, FM phase boundary [12]; ★, AF phase boundary, present work). Filled circles are the p-dependent T_K [11], and the solid lines are guides to the eye. The resistivity is $\sim T^2$ [11] in the shaded part (FL). (b) $S(q, E)$ for $Ce(Ru_{0.24}Fe_{0.76})_2Ge_2$ for $T = 7.5$ K. (c) χ_q for $T = 2.9$ K (◇), 7.5 K (★), and 15.2 K (△). Note the incipient AF order around the (101) Bragg peak ($q = 1.64$ Å^{-1}) at 2.9 K.

The INS experiments were carried out at the IN6 spectrometer at the Institute Laue-Langevin, using an incident neutron wavelength of 5.12 Å. The data were corrected for self-attenuation and neutron absorption, and the magnetic components were separated from the nonmagnetic components using a nonmagnetic reference sample, $LaFe_2Ge_2$. Figure 1(b) shows the resulting dynamic structure factor $S(q, E)$ for $T = 7.5$ K.

The strong scattering found at all q in Fig. 1(b) attests to the intrinsically localized character of the fluctuating moments in $Ce(Ru_{0.24}Fe_{0.76})_2Ge_2$. A quantitative measure of this localized moment is obtained by direct integration of $S(q, E)$ over the experimental E range, yielding $0.8\mu_B$ at 20 K. Since this is a substantial fraction of the $1.74\mu_B$ expected for the ground state of the Ce^{3+} ions [14], we conclude that these moments are long-lived on INS time scales, with a substantial degree of spatial localization at all T.

The strong enhancement of the scattering at the smallest q reveals the presence of long-range correlations among the moments at low T. These correlations are analyzed by extracting χ_q from the experiments by fitting $\chi''(q, E)$ to a modified Lorentzian line shape, described below. The resulting χ_q [Fig. 1(c)] shows two striking features, also evident in $S(q, E)$ [Fig. 1(b)]. First, for all T and $q > 1$ Å^{-1}, χ_q is virtually independent of q. As we show below, the line shape is independent of q in this q range. This q-independent susceptibility reflects the individual response of the magnetic moment of a spatially localized f electron to a fluctuating magnetic field. In fact, this q-independent part completely dominates the local susceptibility $\chi_{\mathrm{loc}}(T)$, which we determine from our data in the standard manner [14]: $\chi_{\mathrm{loc}}(T) = \int \chi_q(T) q^2 dq$. χ_q also shows a pronounced enhancement at small q, which increases with decreasing T. We attribute this to the growth of critical correlations associated with incipient AF order, at the incommensurate propagation vector $Q \sim 0.2 \pm 0.1$ Å^{-1} as implied by the increased scattering observed in our neutron diffraction experiments [15] at satellite positions ($q = 1.56, 1.74$ Å^{-1}) around the (101) Bragg peak.

χ_q shows clear signs of moment compensation by the Kondo effect at the lowest T. $\chi_q(T)$ for representative q values is plotted in Fig. 2(a), including the uniform ($q = 0$) susceptibility $\chi_0(T)$, obtained from a dc susceptibility measurement on a 35 mg piece taken from the INS sample. $\chi_0(T)$ increases with decreasing T, displaying the hallmark power law behavior for

$T < 20$ K found in many nFl systems: $\chi_0(T) = C_0/(T + \theta_W)^{\alpha}$. Here, the Weiss temperature $\theta_W = 0.9 \pm 0.2$ K, $C_0 = (0.87 \pm 0.03)\mu_B^2/\text{meV}^{0.49}$, and $\alpha = 0.51 \pm 0.01$. Since θ_W is nonzero, we see that $\chi_0(T)$ does not truly diverge as $T \to 0$. The absence of divergence is even more evident in $\chi_{\text{loc}}(T)$, which saturates for $T < 5$ K [Fig. 2(a)]. Further evidence for partial Kondo compensation comes from the ~25% reduction in scattered intensity [16] as T is lowered from 20 to 1.9 K [Fig. 2(a)], despite a simultaneous narrowing of the energy linewidth.

The dynamic response in $Ce(Ru_{0.24}Fe_{0.76})_2Ge_2$ is dramatically different from those found in fluctuating moment systems far from a QCP. Like previous INS studies on Kondo lattice systems [14,17–21], the dynamic response in $Ce(Ru_{0.24}Fe_{0.76})_2Ge_2$ is broad and quasielastic. However, Fig. 2(b) shows that the Lorentzian line shape [14,17–21] common to Kondo lattices agrees very poorly with our measured $\chi(q, E)$, both for a small q, where the moments are interacting, and at a large q where the response is purely local. We find instead that at all q and E, for all T from 1.9–200 K, that our data can be satisfactorily described by a simple phenomenological expression: $\chi(q, E) = \chi_q(T)/[1 - iE/\Gamma_q(T)]^{\gamma}$.

The observed line shape is controlled by an energy scale $\Gamma_q(T)$ [22], and by a dynamical exponent $\gamma = 0.15 \pm 0.05$. $\Gamma_q(T)$ extracted from these fits is plotted in Fig. 2(c). For $q = 1.15$ Å^{-1}, Γ_q has the familiar T dependence of a Kondo impurity system, initially decreasing with T before saturating and increasing weakly below T_K, which we identify as ~5 K [22]. Dynamics on this local length scale are consequently not critical. In contrast, Γ_q for $q = 0.35$ Å^{-1} approaches zero with decreasing T, as expected for critical slowing down associated with the $T = 0$ phase transition. With the exception of the lowest T at the larger q, Γ_q is approximately linear in T, $\Gamma_q = \theta_q + a_q T$. The q dependence of θ_q [Fig. 2(d)] demonstrates that dynamic criticality, i.e., $\Gamma_q \to 0$, can be achieved only if $\theta_q \to 0$. For $Ce(Ru_{0.24}Fe_{0.76})_2Ge_2$ this occurs as q approaches the propagation wave vector of incipient AF order, 0.2 ± 0.1 Å^{-1}, the point where $\chi_q(T)$ shows signs of divergence [Fig. 1(c)]. Thus, θ_q is a measure of the distance in q space from the QCP. We conclude that at all T, $\chi(q, E, T)$ is dominated at short length scales by the excitations of individual Kondo moments, while the long wavelength fluctuations become increasingly long-lived and ultimately critical as $T \to 0$.

A random phase approximation (RPA) analysis of $\chi_q(T)$ shows that the singular behavior found near the QCP in $Ce(Ru_{0.24}Fe_{0.76})_2Ge_2$ requires the collaboration of both local and long-range correlations. The long-range correlations are demonstrated in Fig. 3(a): an increasing suppression of χ_{loc}/χ_q is observed at small q on lowering T, signaling the growth of long-range AF correlations. An estimate of the coupling $U_q(T)$, responsible for the

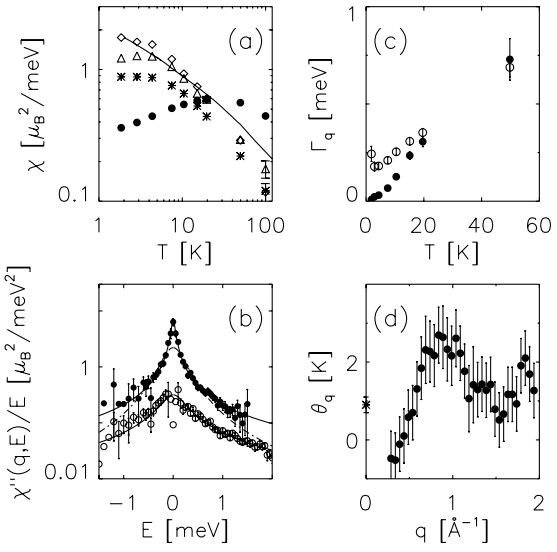

FIG. 2. (a) $\chi_q(T)$, reflecting spatially extended fluctuations probed on length scales $2\pi/q$, shown for $q = 0.35$ Å^{-1} (◇), $q = 0.45$ Å^{-1} (△), and $q = 0$ (solid line). $\chi_{\text{loc}}(T)$ (★) reflects fluctuations localized in real space. Also shown (●, in μ_B^2) is the average of $S_q(T)$ over $1 < q < 1.8$ Å^{-1}, demonstrating the onset of Kondo screening at $T \approx 20$ K. (b) $\chi''(q, E)/E$ for $q = 0.35$ Å^{-1} (●) and $q = 1.15$ Å^{-1} (○, divided by 2 for plotting clarity) at $T = 4.4$ K. The solid lines are the best fits to the modified Lorentzian line shape ($\gamma = 0.15$). The dashed curve is the best fit Lorentzian line shape ($\gamma = 1$). (c) Γ_q of $\chi''(q, E)/E$ for $q = 0.35$ Å^{-1} (●) and $q = 1.15$ Å^{-1} (○). (d) q dependence of the residual linewidth θ_q and θ_W at $q = 0$.

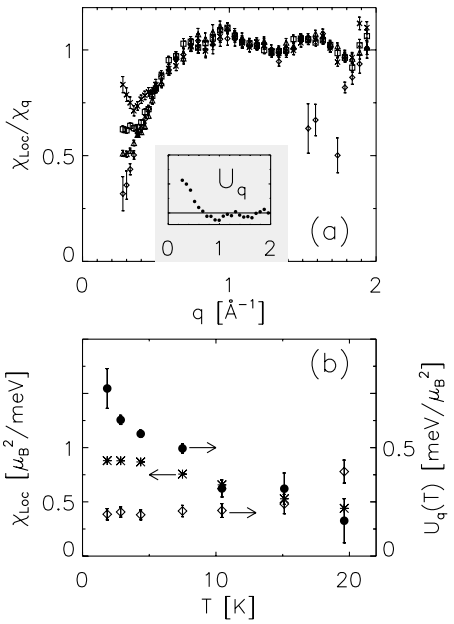

FIG. 3. (a) $\chi_{\text{loc}}(T)/\chi_q(T)$ versus q for $T = 1.9$ K (◇), 4.4 K (△), 7.5 K (□), and 15.2 K (★). This quantity is directly related to the interaction U_q, which is plotted in the inset for $T = 4.4$ K. (b) While the T divergence of χ_{loc} (★) is cut off below ~5 K, $U_{q=0.28}$ (●) increases monotonically to the lowest T. $U_{q=0.55}$ (◇) is T independent.

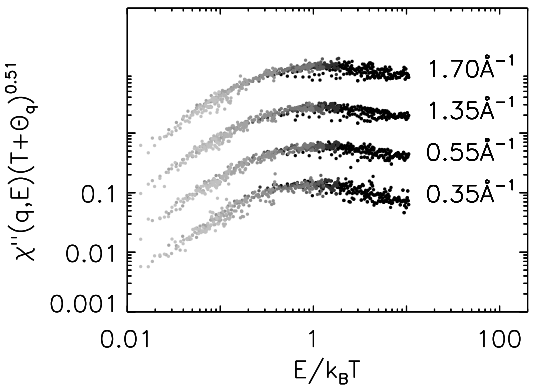

FIG. 4. Scaling of the dynamic response for various q. The INS data $\chi''(q, E)$ have been multiplied by $(T + \theta_q)^{\alpha}$ ($\alpha = 0.51$), and displayed versus E/T with θ_q as in Fig. 2(d). The q values are offset by a factor of 5 along the vertical axis. T ranges from 1.9 K (darkest symbols) to 200 K (lightest symbols). There is substantial overlap in E/T among the 11 T values. Each curve represents ~3000 data points.

formation of long-range correlations, is obtained in the RPA approximation by noting that $\chi_{\rm loc}(T)/\chi_q(T) = 1 - U_q(T)\chi_{\rm loc}(T)$. U_q deduced from this analysis [inset of Fig. 3(a)] demonstrates that the interactions are long ranged, rapidly vanishing for wave vectors larger than ~0.6 Å^{-1}. The T dependence of U_q [Fig. 3(b)] is very different for large and small q. $U_{q=0.55}$ is almost T independent, while $U_{q=0.28}$ increases almost fourfold between 20 and 1.9 K. In contrast, $\chi_{\rm loc}(T)$ initially increases with decreasing T, but ultimately saturates below ~5 K. This RPA analysis reveals that local fluctuations initially provide a bias towards criticality in $Ce(Ru_{0.24}Fe_{0.76})_2Ge_2$, but ultimately it is the intermoment coupling $U_q(T)$ which actually drives the formation of long-range correlations and hence criticality. A similar conclusion was reached for U_2Zn_{17} [20], a heavy fermion AF ($T_N = 9.7$ K). However, neither a departure from Lorentzian line shape, nor any other nFl effects were observed in this system, which is not at a QCP.

The modified Lorentzian introduced above and the observed T linearity of $\Gamma_q(T)$ imply that our data should also display nFl E/T scaling. Interpreting θ_q as the extension to finite q of θ_W, we plot $\chi''(q, E)(T + \theta_q)^{0.51}$ versus E/T in Fig. 4. An excellent collapse of the data taken at different T is observed at each q, spanning 3 orders of magnitude in E/T. The exponent 0.51 is taken from the T dependence of $\chi_0(T)$, as was also found in the locally critical systems UCu_4Pd [9,10] and $CeCu_{5.9}Au_{0.1}$ [7]. Unlike those systems, we find in $Ce(Ru_{0.24}Fe_{0.76})_2Ge_2$ that the dynamical scaling function itself requires a second exponent $\gamma = 0.15$, and that system becomes unstable against fluctuations of wavelength $2\pi/Q$, while remaining stable against disturbances on any other length scale.

Our measurements have established that there are local moments present in $Ce(Ru_{0.24}Fe_{0.76})_2Ge_2$ which become increasingly correlated as $T \to 0$ and which undergo substantial Kondo screening below ~20 K. Although fluctuations of these moments are observed on every length scale, χ_q diverges only at the residual ordering wave vector of the nearby AF phase. The dominance of the long wavelength correlations at the lowest T, and the finite Kondo temperature at the QCP together imply that the $T = 0$ AF transition in $Ce(Ru_{0.24}Fe_{0.76})_2Ge_2$ is a collective instability of the strongly interacting quasiparticles, and is not locally critical. The mean field view of such a phase transition requires diverging length and time scales, leading to Lorentzian line shapes for χ in energy and wave vector. We find instead that $\chi(q, E, T)$ is well described by a modified Lorentzian expression, encompassing the E/T scaling which we observe at every wave vector.

We acknowledge stimulating discussions with P. Coleman, A. J. Millis, and Q. M. Si. MCA thanks T. Gortenmulder and R. Hendrikx for invaluable technical assistance, and acknowledges the hospitality of the MSM group at Leiden. We thank I. P. Swainson for carrying out the neutron diffraction measurements. Work at the University of Michigan was supported by NSF-DMR-997300.

[1] G. R. Stewart, Rev. Mod. Phys. **73**, 797 (2001).
[2] S. Sachdev, *Quantum Phase Transitions* (Cambridge University Press, Cambridge, U.K., 1999).
[3] John A. Hertz, Phys. Rev. B **14**, 1165 (1976).
[4] A. J. Millis, Phys. Rev. B **48**, 7183 (1993); (private communication).
[5] S. Raymond *et al.*, J. Phys. Condens. Matter **13**, 8303 (2001).
[6] P. Coleman, Physica (Amsterdam) **259-261B**, 353 (1999).
[7] A. Schröder *et al.*, Nature (London) **407**, 351 (2000).
[8] Qimiao Si *et al.*, Nature (London) **413**, 804 (2001).
[9] M. C. Aronson *et al.*, Phys. Rev. Lett. **75**, 725 (1995).
[10] M. C. Aronson *et al.*, Phys. Rev. Lett. **87**, 197205 (2001).
[11] S. Süllow *et al.*, Phys. Rev. Lett. **82**, 2963 (1999).
[12] M. B. Fontes *et al.*, Phys. Rev. B **53**, 11678 (1996).
[13] H. Rietschel *et al.*, J. Magn. Magn. Mater. **76–77**, 105 (1988); A. Boehm *et al.*, J. Magn. Magn. Mater. **76–77**, 150 (1988).
[14] B. D. Rainford and S. J. Dakin, Philos. Mag. B **65**, 1357 (1992).
[15] W. Montfrooij *et al.* (unpublished).
[16] N. E. Bickers, D. L. Cox, and J. W. Wilkins, Phys. Rev. B **36**, 2036 (1987).
[17] M. Loewenhaupt *et al.*, J. Phys. (Paris), Colloq. **40**, C4-142 (1979).
[18] G. Aeppli, E. Bucher, and G. Shirane, Phys. Rev. B **32**, 7579 (1985).
[19] A. I. Goldman *et al.*, Phys. Rev. B **33**, 1627 (1986).
[20] C. Broholm *et al.*, Phys. Rev. Lett. **58**, 917 (1987).
[21] U. Walter *et al.*, Phys. Rev. B **36**, 1981 (1987).
[22] For $\gamma = 0.15$ the half width at half maximum (HWHM) and Γ are related by HWHM $= 1.94\Gamma$.